Beam Depletion Spectroscopy of Alkali Atoms (Li, Na, K) Attached to Highly Quantum Clusters

C. Callegari, J. Higgins, F. Stienkemeier,[†] and G. Scoles*

Department of Chemistry, Princeton University, Princeton, New Jersey 08544

Received: April 4, 1997; In Final Form: October 15, 1997[⊗]

We exploit the high efficiency of Langmuir−Taylor surface ionization detectors to measure by beam depletion the electronic absorption spectra of alkali atoms attached to H_2 and He clusters. Li, Na, and K atoms attached to large $(H_2)_N$ and $(D_2)_N$ clusters ($N \approx 10^3-10^4$) have been studied at various ortho/para concentrations in an attempt to correlate the properties of the matrix to the observed spectral features. The results are compared to theoretical predictions and to measurements done by means of conventional matrix isolation spectroscopy in bulk hydrogen. While some similarities are found, several discrepancies remain and are discussed. In the case of helium clusters, beam depletion spectra are very similar to, and in one case identical with, the laser-induced fluorescence spectra measured previously in our laboratory, revealing the total absence of quenching processes. In contrast to this, for alkali atoms attached to hydrogen clusters, quenching processes appear to dominate, and beam depletion spectra are totally different from their laser-induced fluorescence counterparts.

1. Introduction

Van der Waals aggregates or clusters of light atoms or molecules such as He or H_2, whose production was shown possible almost 40 years ago,[1] have recently received an increased amount of attention due to the highly quantum nature of their constituents. The very properties (low atomic mass and weak interatomic forces) that cause bulk He to be liquid down to zero temperature and to exhibit the unique property of superfluidity are expected to play a similar role in the case of clusters. On the other hand, when the size of the cluster is not too large, finite size effects are expected to play a very significant role, and the considerable amount of effort spent to characterize highly quantum clusters can ultimately be seen as an attempt to quantify the finite size scaling of their properties.[2] Finally, because under typical experimental conditions clusters provide an isolated, very low temperature environment which can easily be loaded with a variety of stable and unstable molecules,[3−6] they can be used as a valid complement to bulk phases in matrix isolation spectroscopy.[7,8]

Even if H_2 clusters are easier to produce, the technical requirements to produce He clusters are not prohibitive; as a consequence, more subtle reasons have biased the attention of the scientific community toward the latter system. As we will see in the next sections, He clusters are the most obvious candidate in which to look for superfluidity in finite systems, since they are certainly liquid, whereas only speculations can be made about the actual state of H_2 clusters. Also, computations on He clusters are less demanding than they are for H_2, because He atoms, unlike H_2 molecules, can always be treated as structureless. Finally, He clusters are less perturbative (and colder) substrates for low-temperature spectroscopic investigations of dopant atoms or molecules.

It is not surprising therefore that much more is currently known about He clusters in terms of both theoretical predictions and experimental data, while investigation of H_2 clusters is lagging somewhat behind. The spectroscopic investigation of hydrogen clusters doped with alkali atoms that we report here is a natural extension of our previous work on the spectroscopy of alkali atoms attached to He clusters.[9] Indeed, we partly rely on the much more complete picture that we have of the latter system to interpret our observations for hydrogen clusters. However, while the He study was carried out using laser-induced fluorescence (LIF), the massive amount of quenching present in the case of hydrogen has forced us to use laser-induced beam depletion (LIBD) to detect the alkali's true absorption spectra. This paper reports on LIBD spectra of Li, Na, and K attached on both H_2 and He clusters.

2. Background

2.1. Superfluidity. It is well-known that a two-dimensional ideal boson gas cannot undergo Bose−Einstein condensation.[10] Since Bose−Einstein condensation is a necessary condition for superfluidity, systems of reduced dimensionality are not expected to exhibit superfluidity. Using a more realistic model, Ginzburg and Sobyanin[11] were able to quantify the decrease of the superfluid transition temperature in He for several finite-size geometries. Reducing the size of a system also has the desirable property of lowering its freezing point, because of the increased surface/volume ratio.[2]

These two facts have stimulated a vast amount of experimental and theoretical research on the properties of reduced dimensionality He condensates (e.g. films, adsorbates in porous media, and clusters) which are expected to be liquid at all temperatures (see, for example, refs 2 and 12 for comprehensive reviews). Of particular relevance here is the fact that He clusters as small as 64 atoms have been calculated to show properties associated with superfluidity,[13] and a recent experiment showed the existence of rotons in clusters of several thousand He atoms.[14] However there seems to be a consensus in the scientific community that the existence of *superfluidity* in He clusters will be demonstrated only when quantization of hydrodynamical phenomena is shown to take place.[15]

* Corresponding author. E-mail address: gscoles@princeton.edu.
† Present address: Fakultät für Physik, Universität Bielefeld, D-33615 Bielefeld, Germany.
⊗ Abstract published in *Advance ACS Abstracts,* November 15, 1997.

Molecular hydrogen has been predicted to exhibit superfluidity below 6 K,[16] but such a prediction cannot be verified in the liquid under normal conditions, since the triple point of parahydrogen (p-H_2) lies at a much higher value (13.8 K). A high degree of supercooling is therefore needed; reduction of the system size is essential, to both depress the freezing temperature and reduce the nucleation probability (although an undesirable decrease of the superfluid transition temperature is to be expected[11]). Maris et al.[17,18] were able to supercool H_2 droplets down to only 10.6 K, by levitating them in pressurized liquid He. However, they estimate theoretically that the nucleation rate should fall rapidly below 7 K. This conclusion makes it desirable to cool H_2 as quickly as possible so that a low temperature region is reached where the liquid state is essentially stable. All subsequent attempts to produce supercooled hydrogen have aimed at decreasing the size of the system: hydrogen deposited on a surface[19] or absorbed into Vycor glass[20−24] has been probed without definitive evidence for superfluidity.

Clusters produced in a supersonic expansion at low temperature are the candidate source of supercooled/superfluid hydrogen (ref 25; see ref 3 therein). They are, after formation, completely isolated from any interaction that could cause them to freeze; their final temperature is estimated to be $\approx$4.7 K, and their nucleation times are on the order of 10^{18} s.[26] A number of quantum calculations have been performed on small (p-H_2)$_N$ ($N \leq 135$) clusters[12,27] (earlier ones are reviewed in ref 2). The most relevant finding is that such clusters have a liquidlike structure and exhibit manifestations of superfluid behavior below 2 K, although larger clusters tend to solidify.[25] Typical experiments deal with computationally prohibitive clusters of 10^3 molecules. At such sizes the superfluid transition temperature as well as the freezing temperature will have a somewhat higher value, but clusters will likely be in a metastable liquid state[25] rather than in an equilibrium solid structure. Experiments probing the solid or liquid (possibly superfluid) state of the cluster without destroying it are therefore very desirable; alkali atoms are, a priori, a good candidate probe in view of their simple structure (which simplifies modeling) and their weak interaction with H_2[28] (which prevents them from acting as a nucleation center). As we will see, however, the presence of strong quenching complicates the matter substantially.

2.2. Alkali Atoms in H_2 Clusters and Matrixes. Solid alkali−H_2 mixtures have received considerable attention, in view of their use as rocket fuel,[29] and have triggered a good amount of research including the experiments reported here.

Scharf et al. used path-integral Monte Carlo techniques to calculate the structural properties and absorption spectra of lithium embedded in bulk solid parahydrogen, solid orthodeuterium,[30] parahydrogen clusters and in the bulk liquid.[30] Cheng and Whaley used variational and diffusion Monte Carlo methods to perform the same simulations on pure and Li-doped solid parahydrogen,[32] as well as on pure and Li-doped parahydrogen clusters.[27] Although these algorithms are very efficient and are implemented on increasingly powerful computers, simulations still rely in this specific case on approximate interaction potentials. As a consequence, the results of the two groups present several discrepancies, and a comparison with the available experimental data[33] is also not conclusive at present.

To the best of our knowledge only one experiment on alkali-doped solid hydrogen has been reported in the literature, measuring the absorption spectra of Li in a hydrogen matrix.[33] Commonly known as matrix isolation spectroscopy (MIS), these experiments provide useful information about the interaction energy scale and the nature of trapping sites of the host species but are well-known to suffer from difficulties in making/doping a reproducibly uniform matrix and possibly from the presence of multiple trapping configurations (see refs 33 and 34 for reviews of the subject focused on alkali atoms and/or H_2 matrixes). Clearly, experimental data on simpler systems are needed to test both alkali−H_2 pair potentials (particularly in the excited state) and computational models of alkali-doped H_2 matrixes.

It should also be remembered that nuclear wavefunction symmetry constraints for the H_2 molecule make it necessary to distinguish between o-H_2 (orthohydrogen) and p-H_2 due to their different physical properties. The experiments of ref 33 were carried out exclusively with normal hydrogen, while, as it will be shown later, the o-, p-H_2 relative concentration plays a role in determining the structure of the absorption spectra. Also, simulations have so far been made for pure $J = 0$ (parahydrogen) aggregates only, since they can be treated as spherically symmetric; for molecules in the $J = 1$ state (the lowest state available to o-H_2), orientation would become important and require substantially more complicated modeling.

Large hydrogen clusters present some advantage over conventional matrixes in that they are relatively easy to produce and dope and offer a more homogeneous substrate (the main source of nonhomogeneity being the cluster size distribution). In addition, one can easily change the relative concentration of $J = 0/J = 1$ molecules in the cluster and study its influence on the excitation spectra (and hence on the alkali atom−cluster interaction).

In order not to mislead the reader, we should however remark here that whenever the nature of the substrate is not of concern, He clusters are preferable to H_2 clusters under all respects as a cold matrix to perform spectroscopic studies and have been used for that purpose.[14,35−38] In fact He atoms are more inert than H_2 molecules and have a weaker van der Waals interaction both with each other and with the dopant. As a result, in He clusters a much weaker perturbation is induced on the dopant atom/molecule, and the substrate temperature is lower (0.4 K[6,40,41] vs 4.7 K[26]). Lack of internal structure of the constituents also simplifies spectra of dopants on He clusters, both because inhomogeneous effects are reduced and because fewer inelastic channels (simultaneous excitation of the dopant and of some internal degrees of freedom of the cluster) are available.

2.3. Previous Results and Motivations for the Present Work. Recently, we have been able to obtain the LIF spectra of alkali atoms, dimers, and trimers after attaching them to large He$_N$ clusters ($N \approx 10^4$) using a collisional pick-up doping technique. The spectra of both low spin (e.g. singlet Na$_2$) and high spin (e.g. triplet Na$_2$ and quartet Na$_3$) species have been obtained and analyzed.[9,35−38]

In extending this type of measurement to H_2 clusters, we noted that the fluorescence yield of the alkali atoms in this new environment was 100−1000-fold smaller, and tentatively ascribed this fact to the presence of nonradiative relaxation channels (quenching). It then became obvious that a different measurement scheme, insensitive to the fluorescent yield of the excited dopant, was needed in order to record the total absorption spectra. We therefore implemented a scheme based on the depletion of alkali atoms from the cluster beam induced by laser excitation. A Langmuir−Taylor surface ionization detector was used for this purpose due to its well-known high sensitivity and specificity to alkali atoms.[42]

In principle, LIBD spectra are more likely to reproduce the total absorption spectra of chromophores on He and H_2 clusters,

Beam Depletion Spectroscopy of Li, Na, K

J. Phys. Chem. A, Vol. 102, No. 1, 1998 **97**

because they do not rely on the presence of fluorescent transitions back to the ground state and are therefore insensitive to the wavelength of the emitted fluorescence (which is commonly strongly red-shifted), or to the presence of quenching. LIBD spectra obtained using alkali-doped He clusters are very similar to those obtained by LIF, thus confirming the equivalence of the two techniques when fluorescence detection efficiency is not of concern. In the case of hydrogen, LIF spectra are orders of magnitude weaker than LIBD spectra and are, more importantly, totally different in overall shape, exhibiting a substantially larger amount of structure and a much stronger dependence on the ortho−para composition of the H_2 cluster.

In the present paper we present the LIBD results for both hydrogen and He clusters. While for He the similarity between LIBD and LIF spectra permits an easy comparison to be made, in the case of hydrogen we postpone the presentation of the LIF spectra to a later paper,[50] because they appear to be dominated by the frequency dependence of the quenching processes which is incompletely understood at the present time. On the other hand, we believe that LIBD spectra can be safely assumed to reproduce the overall absorption spectra and as such can be compared to theoretical models and to the helium results.

3. Experiment

No relevant changes have been made to the molecular beam apparatus, which is fully described in previous papers from this group.[9,35,43] Only a brief description with emphasis on the changes necessary to produce hydrogen clusters is given here.

Beams of H_2 or He clusters are prepared by supersonic expansion from a cold nozzle (10 μm diameter, typical stagnation pressure $P_0 = 30$ bar, typical nozzle temperatures $T_0 \approx 70$ K for H_2), resulting in an average size of 10^3 molecules per cluster (this estimate is made by rescaling the value reported in ref 44 with the formula suggested in ref 45). The corresponding values for He are 50 bar, ≈17.5 K, and ≈5000 atoms/cluster. Due to its small diameter, the nozzle orifice is very sensitive to impurities that may deposit on it and alter its effective aperture. To account for this, slightly different source parameters (P_0, T_0) were used for each run, such that the absorption signal was maximized. The exact source parameters for each individual spectrum are reported in the respective figure caption.

An ortho−para converter is used to control the fraction of $J = 1$ hydrogen molecules in the beam. This converter consists of an alumina-supported transition metal catalyst, through which the hydrogen gas supply is passed before reaching the nozzle. Assuming the flux to be slow in comparison to the conversion rate, the ortho−para ratio is determined by the equilibrium thermal distribution at the converter temperature (T_{conv}), which can be set to any value from 300 K down to 20 K. The corresponding $J = 0$ fraction changes from 25% to 99.8% for H_2 (67% to 98% for D_2).

The cluster beam is chopped (for lock-in detection), skimmed, and passed through a pick-up cell where a low (on the order of 10^{-4} mbar) vapor pressure of alkali atoms can be established. Depending on this pressure, each cluster picks up (on average) one or more dopant atoms. Optical excitation spectra of the resulting complexes are obtained by scanning the frequency of a continuous-wave dye or Ti:Al_2O_3 laser, which is fed into the apparatus through a single mode fiber. The laser beam crosses the cluster beam perpendicularly a few centimeters after the pick-up cell, at the center of a laser-induced fluorescence detector equipped with a photomultiplier tube (PMT, Thorn-EMI 9863QB). A Langmuir−Taylor surface ionization detector

using rhenium as an ionizing filament is located further downstream of the cluster beam. Alkali atoms hitting the filament are ionized, collected by a surrounding grid, and detected as a macroscopic current.

Electronic excitation results in a decrease of the beam-correlated alkali flux. Let us discuss the mechanisms contributing to this effect within the framework of the model developed in ref 9 (i.e. treating the chromophore−cluster complex as a diatomic molecule). There are, in principle, three possibilities:

(1) The chromophore directly evaporates from the cluster after excitation (i.e. we have a bound−free transition to the repulsive wall of the upper state potential) and fluoresces back to its ground state as a free atom.

(2) The chromophore remains bound to the cluster after excitation, but is evaporated in the de-excitation process. While in ref 9 we tentatively proposed a rearrangement of the whole cluster followed by a bound−free de-excitation transition to the repulsive wall of the ground state to explain the experimental dispersed fluorescence profiles, very recent time-resolved investigations of Na on He clusters suggest the formation and evaporation of a Na^*−He excimer[46] followed by red-shifted fluorescent emission.

(3) The chromophore is excited in a bound−bound transition and remains bound also after de-excitation (for instance when the chromophore location is inside the cluster). In this case the de-excitation may produce substantial evaporation and, as a consequence, an increase in the angular dispersion of the cluster beam. This produces a (smaller) decrease in the flux of alkali atoms carried by the clusters to the Langmuir−Taylor detector.

As already pointed out, LIBD detection offers information that is complementary to LIF, because it is sensitive also to atoms whose fluorescence might be quenched or red-shifted beyond the detection limit of the PMT tube. As an example we show in Figure 1a the LIBD and LIF spectra for Li attached to H_2 clusters containing ≈10^3 atoms. Note the negligible amount of fluorescence generated by excitation to the red of the gas-phase lines, where most of the absorption is located in the case of the LIBD spectra.

4. Results

4.1. Li Atoms Attached to Hydrogen Clusters. Since experimental results obtained by matrix isolation and theoretical calculations are available for comparison, we first focus on the spectra of lithium attached to hydrogen clusters.

Figure 1 shows the LIBD spectra of Li attached to hydrogen clusters. Clusters are grown with hydrogen close to normal composition (upper panel), parahydrogen (middle) or deuterium of normal composition (lower panel). [The denominations para and ortho are used for clusters grown from hydrogen mixtures consisting mostly of the corresponding J-state. The exact fractions of $J = 0$ and $J = 1$ molecules are specified in the figures.] The vertical line shows the position of the atomic gas phase $2^2P_{3/2}, 2^2P_{1/2} \leftarrow 2^2S_{1/2}$ transitions, which are unresolved on the scale of the plot. We note that the width and position of the main absorption maximum is roughly the same for all three substrates. Some differences are seen in the positions and amplitudes of the blue-shifted maxima.

The use of clusters for spectroscopic investigation of unusual species[35−37] or of the host−guest interaction in doped systems[9,14,37,41,44] is still very young, and only a handful of results are available for comparison. MIS, the equivalent of cluster spectroscopy in bulk materials, is a venerable technique (for a review, see refs 47−49 and references therein), and most of its
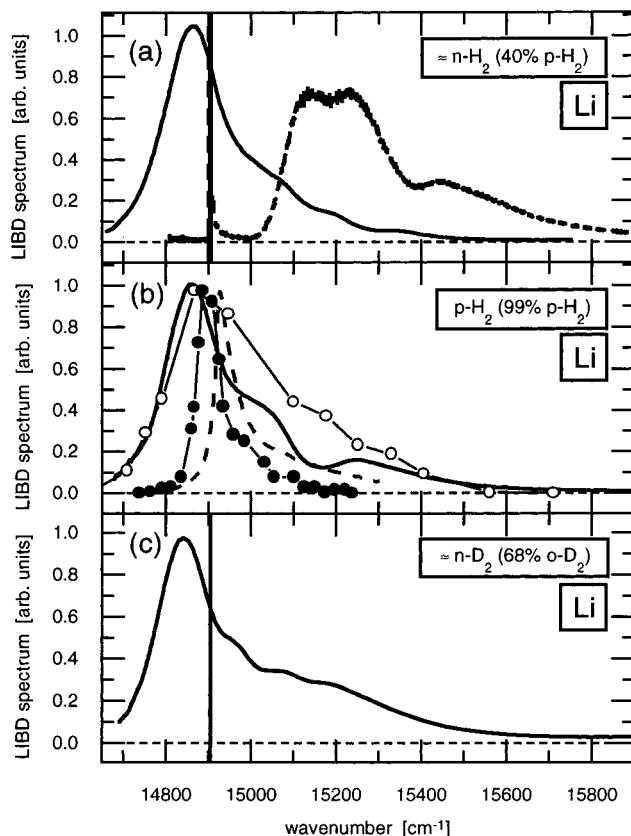
Figure 1. (a) Laser induced beam depletion spectrum (thin solid line) and laser induced fluorescence spectrum (thick dashed line) of lithium atoms attached to $\approx n\text{-}H_2$ clusters (40% $p\text{-}H_2$). (b) LIBD spectrum of Li atoms attached to $p\text{-}H_2$ clusters (thick solid line), compared with different theoretical simulations: Li on the surface of a $(p\text{-}H_2)_{33}$ cluster (●, from ref 30), Li on the surface of a $(p\text{-}H_2)_{134}$ cluster (dashed line, from ref 27), and Li inside bulk liquid $p\text{-}H_2$ (○, from ref 30). (c) LIBD spectrum of Li atoms attached to D_2 clusters. In panels a and c the vertical bar marks the position of the atomic gas phase $2^2P_{1/2}$, $2^2P_{3/2}$ ← $2^2S_{1/2}$ transitions, whose separation (0.34 cm^{-1}) is unresolved on the scale of the plot. Experimental conditions are (see the experimental section for notation) (a) $P_0 = 31$ bar, $T_0 = 85$ K, $T_{conv} = 100$ K; (b) $P_0 = 31$ bar, $T_0 = 85$ K, $T_{conv} = 25$ K; and (c) $P_0 = 31$ bar, $T_0 = 70$ K, $T_{conv} = 100$ K.

findings can be related to the cluster case. In particular, it is well-established that the presence of a split absorption profile is a signature of the 3-fold degeneracy of the alkali p-state being lifted by a nonspherically symmetric environment. The presence of more than three peaks has been ascribed to the existence of different substitutional sites inside the lattice. As the size of the site decreases, the center of gravity of the triplet is shifted more to the blue relative to the free atom absorption, in agreement with the naïve particle-in-the-box model. Red-shifted absorption peaks have also been observed that have been associated with relatively large trapping sites.

In the specific case of Li in H_2, the calculations of Cheng and Whaley always predict blue-shifted spectra in the bulk solid,[32] irrespective of the size of the trapping cavity (1−13 vacancies), and minimally blue-shifted spectra[27] for surface atoms. One would then conclude that the position of the peaks in the absorption spectra could be used to easily determine whether the chromophore is located inside or on the surface of the cluster. Unfortunately, Scharf et al.[30] predict almost no shift both for atoms on the surface of H_2 clusters and atoms in bulk liquid H_2. Matrix spectra by Fajardo[33] (where any doubt about the location of the chromophores inside the solid lattice is eliminated by coating the surface with neon) also show a

moderate red-shift rather than a large blue shift. The large blue shift in Cheng and Whaley's calculations probably originates from neglecting the increase in polarizability of the excited lithium atom (i.e. the change in the C_6 coefficient of the Li−H_2 interaction potentials). Therefore the positions of the peaks alone do not seem to offer conclusive information on the location of the chromophore.

The models used in refs 30 and 32 show a much better agreement in predicting the width of the absorption profile of Li atoms on the surface of a cluster (60−70 cm^{-1}), and both find this configuration energetically more favorable than the atom solvated inside the cluster. Of particular interest is that even when the initial configuration has the Li atom at the center of the cluster, the diffusion Monte Carlo procedure in ref 27 leads to a surface location of the dopant when equilibrium is reached. Although in the experiment the Li atoms might go inside the cluster immediately after the pick-up event, the cluster travels for a relatively long time ($\lesssim 100$ μs) between doping and laser excitation. This time is likely to be sufficient for the migration of the dopant to the surface. We note that our absorption profiles are narrower than those of the calculated and experimental bulk spectra but broader than those calculated for the surface spectra. This is not in contrast to locating the Li atoms on the surface of the cluster, because the additional broadening may well arise from mechanisms not accounted for by theory, such as the simultaneous excitation of internal modes of the cluster. Furthermore, since quenching of radiative transitions might be dominant in alkali-doped hydrogen clusters,[50] lifetime broadening might also contribute to the width of the observed spectra. Finally, we want to observe that the model of Scharf et al. shows little difference between the absorption spectra of Li in the bulk liquid or in a solid matrix; therefore, because of limitations in the present level of theoretical understanding, our spectra are unsuitable in deciding on the aggregation state of the clusters.

Calculations[30] and absorption measurements[33] carried out on deuterium matrixes show an intensified blue wing absorption band with respect to the H_2 case. We observe the same trend when comparing the spectrum of Li on H_2 clusters with the spectrum of Li on D_2 (Figure 1). Because of its lower zero point energy, deuterium is denser and more tightly bound than hydrogen. This should increase the repulsive interaction with the excited Li atom and hence increase the probability of bound−free (blue-shifted) transitions.

The influence on the LIBD spectra of the ortho−para concentration in the clustering gas (compare the top and middle panels of Figure 1) is not very large; it is much more pronounced in the LIF measurements and will be discussed in a forthcoming paper.[50] As pointed out by one of the reviewers, at the highest levels of purity presented in our experiment (99% $p\text{-}H_2$, 1% $o\text{-}H_2$) there are still enough $o\text{-}H_2$ molecules to form a more stable "solvent shell" around the dopant atom, in the assumption that $o\text{-}H_2$ interacts more strongly with alkali atoms. As an effect, large changes in the ortho−para composition of the cluster would induce only minor changes in the local environment of the alkali atom, which would be consistent with the relatively small changes observed in our experiments. We are not aware of any calculation of the interaction of alkali atoms with hydrogen molecules in specific rotational states. Such data are available for the H_2 −H_2 interaction,[51] for which the binding energies do not change appreciably with the rotational state (2.85 cm^{-1} for the $J = 0/J = 0$ pair, 2.87 cm^{-1} for the $J = 0/J = 1$ pair); similarly, the parameters governing the interaction (polarizability, electric quadrupole moment) are almost unchanged
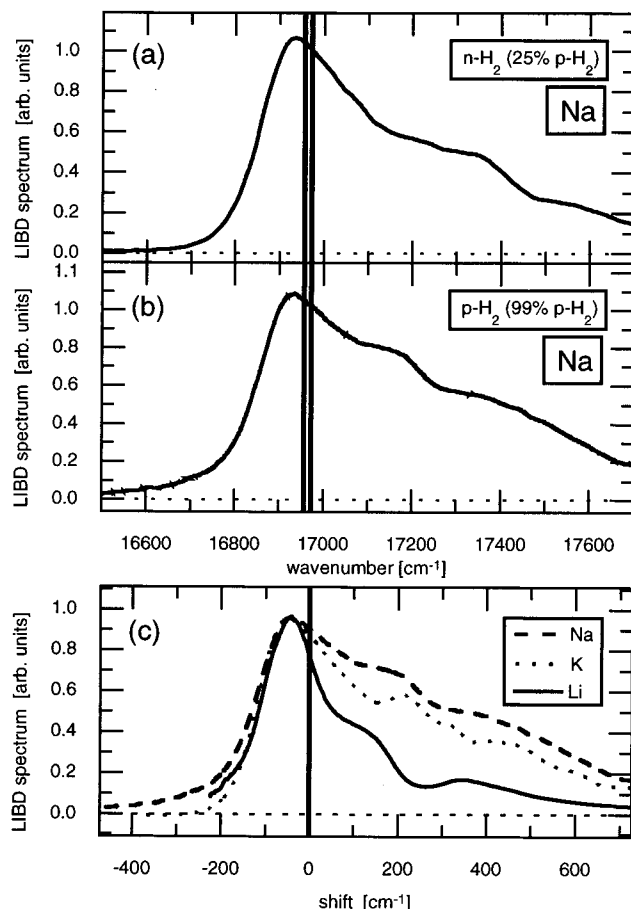
Beam Depletion Spectroscopy of Li, Na, K

J. Phys. Chem. A, Vol. 102, No. 1, 1998 **99**

Figure 2. (a, b) Laser induced beam depletion spectra of sodium attached to hydrogen clusters at different ortho−para fractions. (c) Comparison of LIBD spectra for Li, Na, and K on p-H_2 clusters (shifts are relative to the $^2P_{3/2} \leftarrow {}^2S_{1/2}$ transition. As in Figure 1 the vertical bar(s) mark the position(s) of the atomic gas-phase transition(s). Experimental conditions are (a) $P_0 = 31$ bar, $T_0 = 70$ K, no converter installed; (b) $P_0 = 31$ bar, $T_0 = 60$ K, $T_{conv} = 25$ K; and (c) see Figures 1b, 2b, 3b.

Figure 3. (a, b) Laser induced beam depletion spectra of potassium attached to hydrogen clusters at different ortho−para fractions. (c) LIBD spectrum of K atoms attached to D_2 clusters. As in Figure 1 the vertical bars mark the positions of the atomic gas-phase transitions. Experimental conditions are (a) $P_0 = 29$ bar, $T_0 = 70$ K, no converter installed; (b) $P_0 = 31$ bar, $T_0 = 60$ K, $T_{conv} = 40$ K; (c) $P_0 = 31$ bar, $T_0 = 70$ K, $T_{conv} = 40$ K.

($\approx 0.2\%$ increase going from the $J = 0$ to the $J = 1$ state[52]). Extrapolating to the alkali−H_2 case, we do not expect that a "solvent shell" will be formed around the alkali atom, on the basis of the change of the alkali−H_2 interaction alone. It is however known[52] that $J = 1$ hydrogen molecules diluted in a $J = 0$ matrix tend to pair, with a gain in energy of ≈ 2.4 cm^{-1}. In bulk p-H_2, massive clustering of diluted $J = 1$ impurities is not an issue because characteristic diffusion times may be hours. In a cluster, due to the enhanced mobility at the surface and to the (possibly) liquid state of the cluster, the possibility exists that the $J = 0$ and $J = 1$ fractions undergo a phase separation, with the alkali atom preferably remaining with the $J = 1$ phase. We do not know if this is the case; we would only like to point out that the intensity of a selected peak in our LIF spectra shows an almost linear dependence on the percentage of o-H_2 in the clustering gas; the hypothesis of a preferred "solvent shell" is not likely to be consistent with this finding.

4.2. Na and K Attached to Large Hydrogen Clusters. The absorption profiles of sodium and potassium atoms attached to hydrogen clusters are shown in Figures 2 and 3. Again the two vertical lines indicate the position of the atomic gas-phase transitions. For Na the spectrum on D_2 clusters was not obtained. Although the broadening and splitting of the absorption features increases somewhat for the heavier dopants (as commonly observed in MIS)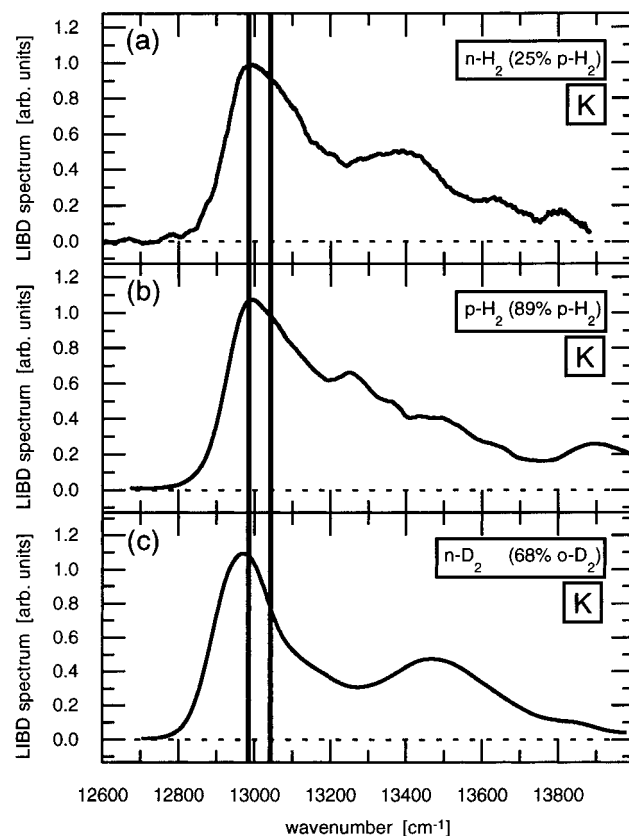, the general pattern of the spectra remains the same. Furthermore, if the spectra are displayed in such a way that all $P_{3/2}$ lines coincide, one finds that the absolute maxima are red-shifted by the same amount (see panel c in Figure 2). As already observed with Li, the red shift of the main peak for K/D_2 is larger than for K/H_2.

On the basis of the similarities of their spectra with those of Li, one would say that Na and K also reside on the surface of the clusters. On the other hand, we have seen that red-shifted peaks are observed in "bulk" spectra as well, the main difference with "surface" spectra being the width of the peaks. Unfortunately, for Na and K no simulations or matrix spectra are available for direct comparison. It should be remarked that according to the prediction of Ancilotto et al.,[53] Na and K are readily solvated by liquid H_2, but those results rely on Na−H_2 and K−H_2 potentials that have been calculated with a different technique than those for Li−H_2. It is interesting to observe that large differences exist in the estimated value of the alkali−H_2 potential well depth (D_e), depending on the calculation scheme,[28,54,55] but within the same scheme the ordering $(D_e)_{Li} > (D_e)_{Na} > (D_e)_K$ always holds. It is therefore not unreasonable to assume that if the most strongly interacting alkali atom (Li) has a stable surface state (as we claimed before), Na and K do as well. Variations in the position and appearance of the blue-shifted maxima related to the composition of the cluster are also observed for Na and K (Figures 2 and 3). As in the case of Li, these effects are much more evident in the fluorescence spectra and will be discussed in ref 50.

4.3. Beam Depletion Spectra of Alkali Atoms Attached to Superfluid Helium Droplets. In a previous paper by our
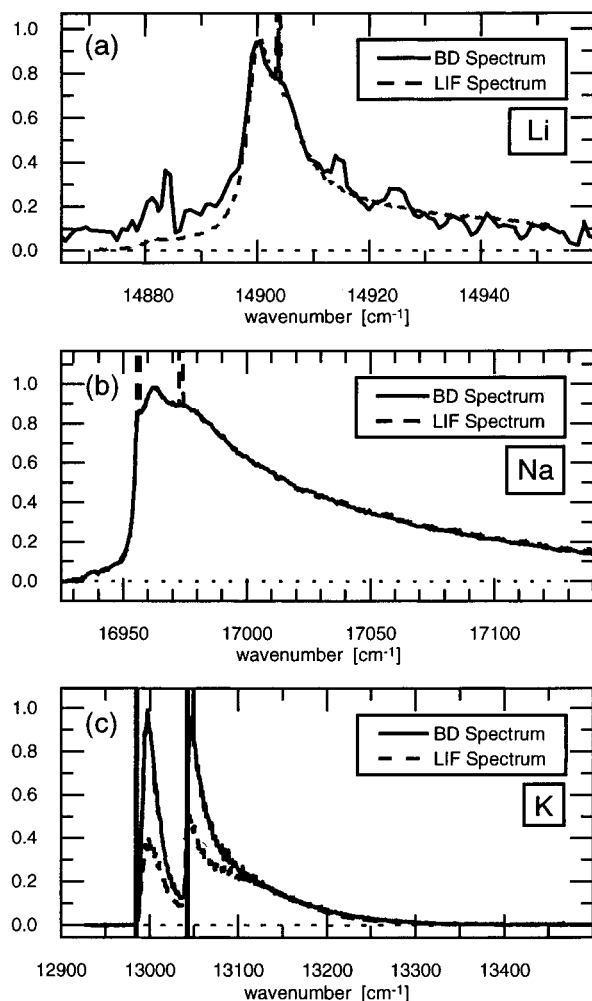
Figure 4. Laser induced beam depletion spectra of alkali atoms (Li, Na, and K) attached to liquid helium droplets. Included in plots a and c are the Laser induced fluorescence spectra from ref 9 normalized in height. The spectra in b are recorded simultaneously; contrary to all other spectra, they are not corrected for laser intensity. Experimental conditions are (a-LIF) $P_0 = 52$ bar, $T_0 = 17.5$ K; (a-LIBD) $P_0 = 55$ bar, $T_0 = 17.5$ K; (b) $P_0 = 50$ bar, $T_0 = 20.0$ K; (c-LIF) $P_0 = 52$ bar, $T_0 = 18.9$ K; (c-LIBD) $P_0 = 52$ bar, $T_0 = 18.6$ K.

group[9] laser-induced excitation and emission spectra of Li, Na, and K attached to large helium clusters have been reported and explained. From the shape and position of the absorption profiles it was already clear that the dopant atoms reside on the surface of the cluster rather than being solvated inside. Calculations within a static molecular model and the measured emission spectra gave us a conclusive picture of the binding of the alkali atom to the surface of the He droplet and of the dynamics of the processes induced by the excitation. In particular, bound−bound and bound−free transitions could be discriminated both in the model and in the experimental observations. Even though nonradiative transitions are not expected to play a relevant role, direct proof that the LIF spectra are equivalent to the absorption spectra was not obtained at that time. LIBD spectra, being complementary to LIF, allow us to establish this equivalence.

The recorded spectra are shown in Figure 4, along with the LIF spectra from ref 9, which are included for comparison. In the case of Na, a recent improvement of the experimental setup has allowed for the LIF and LIBD spectra to be recorded simultaneously (panel b), thus guaranteeing the same experimental conditions.[56] Except for the intense fluorescence signal at the atomic gas-phase lines position (originating from the

presence of background sodium vapor in the chamber where the LIF detector is located), no significant differences are observed between LIF and LIBD spectra, which are almost indistinguishable in the figure. This confirms that quenching is negligible.

LIF and LIBD spectra of Li also match within the errors which are in this case larger and are due to the noisy surface ionization detection of Li atoms. The LIF and LIBD spectra recorded for K (Figure 4, lowermost panel) exhibit large differences. Such differences can be ascribed to the nonuniform detection efficiency of the PMT, which overemphasizes the contribution of the bound−free transitions. In fact, the fluorescence from both free and bound K atoms falls on the red tail of the PMT response curve, and as a result, the PMT quantum efficiency at the position of the K gas-phase lines ($\approx$13 000 cm^{-1}) is twice as large as the quantum efficiency at the average emission frequency of a K*−He excimer ($\approx$12 000 cm^{-1}). In order to compensate for this effect, one has to calculate the "true signal", $S(f)$, at each excitation frequency in terms of the measured signal, $s(f)$, as

$$S(f) = \frac{s(f) \int \frac{\varphi(f,f')}{\epsilon(f')} \, df'}{\int \varphi(f,f') \, df'} \quad (1)$$

where $\varphi(f,f')$ is the measured *emission* spectrum as a function of the excitation (f) and emission (f') frequencies, and $\epsilon(f')$ is the frequency-dependent quantum efficiency of the PMT.[57] Since an emission spectrum needs to be collected at each excitation frequency, only a limited set of data points has been analyzed and found to support the hypothesis that LIF spectra, once compensated for detection efficiency, would be the same as LIBD spectra also in the case of K.

5. Conclusions

Large hydrogen/deuterium clusters have been produced in a supersonic beam and doped with alkali atoms. Laser-induced fluorescence is shown to be inadequate to measure the total absorption spectra of such complexes, due to the overwhelming presence of nonradiative channels for relaxation of the excited chromophore. A beam depletion detection scheme making use of a Langmuir−Taylor probe has been proven to be a valid tool to obtain the absorption spectra of Li, Na, and K attached to H_2 and D_2 clusters which are reported here for the first time. Hydrogen clusters are shown to be a valid complement to conventional matrix isolation spectroscopy, since they are immune to most of its drawbacks. Agglomeration of the dopants into dimers or larger entities, degeneration of the probed material in time, coverage variations at the surface, and substrate nonuniformity are of much less concern when using clusters. Also, clusters are easier to prepare and their ortho−para composition can be easily varied, so that the influence of the rotational state of the hydrogen molecules can be studied. Most importantly, clusters of almost pure $J = 0$ hydrogen can be prepared and compared to calculations (which to date have been carried out exclusively on the $J = 0$ state of H_2 and D_2). Interaction potentials and computational capabilities are at present inadequate to correctly model the systems studied here, and the observed spectra are not completely understood. Basic properties of the system, such as the location of the impurity, the size of the trapping site, and the aggregation state of the cluster cannot be safely predicted on the basis of existing simulations. We hope that the data presented here can further

Beam Depletion Spectroscopy of Li, Na, K

J. Phys. Chem. A, Vol. 102, No. 1, 1998 **101**

stimulate computational activity on the subject, so that some of the open questions are finally answered.

LIBD spectra of alkali on *helium* clusters confirm LIF as a suitable technique to measure the absorption of these complexes. We find no differences in the spectra taken with the two detection methods, except when potassium is used as a dopant. We consider this anomaly an instrumental artifact due to the nonuniform frequency response of the PMT in the spectral region of concern.

References and Notes

(1) Becker, E. W.; Klingelhöfer, R.; Lohse, P. *Z. Naturforsch. A: Astrophys., Phys., Phys. Chem.* **1961**, *16A*, 1259.

(2) Whaley, K. B. *Int. Rev. Phys. Chem.* **1994**, *13*, 41.

(3) Gough, T. E.; Mengel, M.; Rowntree, P. A.; Scoles, G. *J. Chem. Phys.* **1985**, *83*, 4958.

(4) Goyal, S.; Schutt, D. L.; Scoles, G. *Phys. Rev. Lett.* **1992**, *69*, 933.

(5) Scheidemann, A.; Toennies, J. P.; Northby, J. A. *Phys. Rev. Lett.* **1990**, *64*, 1899.

(6) Gspann, J. *Z. Phys. B: Condens. Matter* **1995**, *98*, 405, and references therein.

(7) Goyal, S.; Schutt, D. L.; Scoles, G. *J. Chem. Phys.* **1995**, *102*, 2302.

(8) Higgins, J.; Callegari, C.; Reho, J.; Stienkemeier, F.; Ernst, W. E.; Scoles, G. Manuscript in preparation.

(9) Stienkemeier, F.; Higgins, J.; Callegari, C.; Kanorsky, S. I.; Ernst, W. E.; Scoles, G. *Z. Phys. D: At., Mol. Clusters* **1996**, *38*, 253.

(10) See for example: Agarwal, B. A.; Eisner M. *Statistical Mechanics*; Wiley Eastern Ltd: New Delhi, 1988; p 149.

(11) Ginzburg V. L.; Sobyanin, A. A. *Sov. Phys. Usp. (Engl. Transl.)* **1976**, *19*, 773.

(12) Cheng, E.; McMahon, M. A.; Whaley, K. B. *J. Chem. Phys.* **1996**, *104*, 2669. Rama Krishna, M. V.; Whaley, K. B. *J. Chem. Phys.* **1990**, *93*, 746. Rama Krishna, M. V.; Whaley, K. B. *Phys. Rev. Lett.* **1990**, *64*, 1126.

(13) Sindzingre, P.; Klein, M. L.; Ceperley D. M. *Phys. Rev. Lett.* **1989**, *63*, 1601.

(14) Hartmann, M.; Mielke, F.; Toennies, J. P.; Vilesov, A. F.; Benedek, G. *Phys. Rev. Lett.* **1996**, *76*, 4560.

(15) III. Workshop on Quantum Fluid Clusters, June 15−18, 1997, Schloss Ringberg, Germany; organized by Toennies J. P., and Whaley K. B.

(16) Ginzburg, V. L.; Sobyanin, A. A. *JETP Lett. (Engl. Transl.)* **1972**, *15*, 242.

(17) Seidel, G. M.; Maris, H. J.; Williams, F. I. B.; Cardon, J. G. *Phys. Rev. Lett.* **1986**, *56*, 2380.

(18) Maris, H. J.; Seidel, G. M.; Williams, F. I. B. *Phys. Rev. B: Condens. Matter* **1987**, *36*, 6799.

(19) Vilches, O. E. *J. Low Temp. Phys.* **1992**, *89*, 267.

(20) Bretz, M.; Thomson, A. L. *Phys. Rev. B: Condens. Matter* **1981**, *24*, 467.

(21) Torii, R. H.; Maris, H. J.; Seidel, G. M. *Phys. Rev. B: Condens. Matter* **1990**, *41*, 7167.

(22) Brewer, D. F.; Rajendra, J. C. N.; Thomson, A. L. *Phys. B (Amsterdam)* **1994**, *194*, 687.

(23) McClintock, P. *Phys. World* **1995**, *8*, 23.

(24) McClintock, P. *Phys. World* **1995**, *8*, 31.

(25) Sindzingre, P.; Ceperley, D. M.; Klein, M. L. *Phys. Rev. Lett.* **1991**, *67*, 1871.

(26) Knuth, E. L.; Schünemann, F.; Toennies, J. P. *J. Chem. Phys.* **1995**, *102*, 6258.

(27) Cheng, E.; Whaley, K. B. *J. Chem. Phys.* Submitted.

(28) Rossi, F.; Pascale, J. *Phys. Rev. A: Gen. Phys.* **1985**, *32*, 2657.

(29) Carrick, P. In *High Energy Density Matter Contractors Conference, Woods Hole, MA, 1993*; Edwards Air Force Base: Edwards, CA, 1993; p 412.

(30) Scharf, D.; Martyna, G. J.; Li, D.; Voth, G. A.; Klein, M. L. *J. Chem. Phys.* **1993**, *99*, 9013.

(31) Scharf, D.; Martyna, G. J.; Klein, M. L. *J. Chem. Phys.* **1993**, *99*, 8997.

(32) Cheng, E.; Whaley, K. B. *J. Chem. Phys.* **1996**, *104*, 3155.

(33) Fajardo, M. E. *J. Chem. Phys.* **1993**, *98*, 110.

(34) Tam, S.; Fajardo, M. E. *Chem. Phys.* **1993**, *189*, 351.

(35) Stienkemeier, F.; Ernst, W. E.; Higgins, J.; Scoles, G. *J. Chem. Phys.* **1995**, *102*, 615.

(36) Stienkemeier, F.; Ernst, W. E.; Higgins, J.; Scoles, G. *Phys. Rev. Lett.* **1995**, *74*, 3592.

(37) Higgins, J.; Callegari, C.; Reho, J.; Stienkemeier, F.; Ernst, W. E.; Lehmann, K. K.; Gutowski, M.; Scoles, G. *Science (Washington, D.C.)* **1996**, *273*, 629.

(38) Higgins, J.; Ernst, W. E.; Callegari, C.; Reho, J.; Lehmann, K. K.; Scoles, G.; Gutowski, M. *Phys. Rev. Lett.* **1996**, *77*, 4532.

(39) Bartelt, A.; Close, J. D.; Federmann, F.; Quaas, N.; Toennies, J. P. *Phys. Rev. Lett.* **1996**, *77*, 3525.

(40) Brink, D. M.; Stringari, S. *Z. Phys. D: At., Mol. Clusters* **1990**, *15*, 257.

(41) Hartmann, M.; Miller, R. E.; Toennies, J. P.; Vilesov, A. *Phys. Rev. Lett.* **1995**, *75*, 1566.

(42) Persky, A.; Greene, E. F.; Kuppermann, A. *J. Chem. Phys.* **1968**, *49*, 2347.

(43) Goyal, S.; Schutt, D. L.; Scoles, G. *J. Phys. Chem.* **1993**, *97*, 2236.

(44) Schutt, D. L. *Ph.D. Thesis*; Princeton University: Princeton, NJ, 1992.

(45) Haberland, H. In *Clusters of Atoms and Molecules: Theory, experiment, and clusters of atoms (Springer series in chemical physics; v. 52)*; Haberland, H., Ed.; Springer-Verlag: New York, 1994; p 221.

(46) Reho, J.; Callegari, C.; Higgins, J.; Ernst, W. E.; Lehmann, K. K.; Scoles G. *Faraday Discuss. Chem. Soc.* **1997**, *108*, in press.

(47) Boatz, J. A.; Fajardo, M. E. *J. Chem. Phys.* **1994**, *101*, 3472.

(48) Fajardo, M. E.; Carrick, P. G.; Kenney, J. W., III *J. Chem. Phys.* **1991**, *94*, 5812.

(49) Tam, S.; Fajardo, M. E. *J. Chem. Phys.* **1993**, *99*, 854.

(50) Callegari, C.; Stienkemeier, F.; Higgins, J.; Scoles, G. Manuscript in preparation.

(51) Schaefer J. *Astron. Astrophys.* **1994**, *284*, 1015.

(52) Silvera, I. F. *Rev. Mod. Phys.* **1980**, *52*, 393.

(53) Ancilotto, F.; Cheng, E.; Cole, M. W.; Toigo, F. *Z. Phys. B: Condens. Matter* **1995**, *98*, 323.

(54) Scoles, G. *Int. J. Quantum Chem.* **1990**, *24*, 475.

(55) Chaban, G.; Gordon, M. S. *J. Phys. Chem.* **1996**, *100*, 95.

(56) The improvement consists of locating the surface ionization detector in a separately pumped chamber and collecting the ions with an electron multiplier. This results in lower background and increased sensitivity for LIBD measurements; it also allows simultaneous collection of LIF and LIBD spectra, since the light emitted by the surface ionization detector hot wire does not affect the photomultiplier. This configuration has been adopted both at Princeton and in a new apparatus built by Frank Stienkemeier in Bielefeld, giving identical results.

(57) Electron Tubes Ltd., *Photomultiplier Tubes Catalog*, 1996.